THE JOURNAL OF BIOLOGICAL CHEMISTRY VOL. 288, NO. 47, pp. 33745–33759, November 22, 2013

New Hyperekplexia Mutations Provide Insight into Glycine Receptor Assembly, Trafficking, and Activation Mechanisms*

Received for publication, August 10, 2013, and in revised form, October 1, 2013 Published, JBC Papers in Press, October 9, 2013, DOI 10.1074/jbc.M113.509240

Anna Bode,[a1] Sian-Elin Wood,[b1] Jonathan G. L. Mullins,[b] Angelo Keramidas,[a] Thomas D. Cushion,[b] Rhys H. Thomas,[b,c] William O. Pickrell,[b,c] Cheney J. G. Drew,[b,c] Amira Masri,[d] Elizabeth A. Jones,[e,f] Grace Vassallo,[g] Alfred P. Born,[h] Fusun Alehan,[i] Sharon Aharoni,[j,k] Gerald Bannasch,[l] Marius Bartsch,[m] Bulent Kara,[n] Amanda Krause,[o] Elie G. Karam,[p] Stephanie Matta,[p] Vivek Jain,[q] Hanna Mandel,[r] Michael Freilinger,[s] Gail E. Graham,[t] Emma Hobson,[u] Sue Chatfield,[v] Catherine Vincent-Delorme,[w] Jubran E. Rahme,[x] Zaid Afawi,[y] Samuel F. Berkovic,[z] Owain W. Howell,[b,c] Jean-François Vanbellinghen,[aa] Mark I. Rees,[b,c] Seo-Kyung Chung,[b,c2] and Joseph W. Lynch[a3]

From the [a]University of Queensland, Queensland Brain Institute and School of Biomedical Sciences, Queensland 4072, Australia, [b]Department of Neurology Research and Molecular Neuroscience, Institute of Life Science, College of Medicine and the [c]Wales Epilepsy Research Network, College of Medicine, Swansea University Swansea SA2 8PP, United Kingdom, the [d]Department of Paediatrics, Division of Child Neurology, Faculty of Medicine, University of Jordan, Amman 11942, Jordan, the [e]Manchester Centre for Genomic Medicine and the [g]Royal Manchester Children's Hospital, Central Manchester University Hospitals National Health Service Foundation Trust, Manchester Academic Health Sciences Centre, Manchester M13 9WL, United Kingdom, the [f]Manchester Centre for Genomic Medicine, Institute of Human Development, Faculty of Medical and Human Sciences, University of Manchester, Manchester Academic Health Sciences Centre, Manchester M13 9WL, United Kingdom, the [h]Department of Pediatrics, Copenhagen University Hospital, Rigshospitalet, 2100 Copenhagen, Denmark, the [i]Department of Pediatrics, Division of Child Neurology, Faculty of Medicine, Başşkent University, 06990 Ankara, Turkey, the [j]Institute of Pediatric Neurology, Schneider Children's Medical Center of Israel, Petah Tikva 49202, Israel, the [k]Sackler Faculty of Medicine, Tel Aviv University, Tel Aviv 69987, Israel, the [l]Neurology Department, Affinity Medical Group, Menasha, Wisconsin 54952, the [m]Department of Neonatology, University Medical Center of the Johannes Gutenberg University Mainz, D-55099 Mainz, Germany, [n]Kocaeli University Medical Faculty, Department of Pediatrics, Division of Child Neurology, 41380 Kocaeli, Turkey, the [o]Division of Human Genetics, National Health Laboratory Service, and School of Pathology, Faculty of Health Sciences, University of the Witwatersrand, 2000 Johannesburg, South Africa, the [p]Department of Psychiatry and Clinical Psychology, Saint George Hospital University Medical Center, Balamand University, Faculty of Medicine, Beirut 1100 2807, Lebanon, the [q]Royal Children's Hospital Melbourne, Children's Neuroscience Centre, Royal Children's Hospital, Victoria 3052, Australia, the [r]Metabolic Unit, Meyer Children's Hospital, Rambam Medical Center, Technion Faculty of Medicine, Haifa 31096, Israel, the [s]Department of Pediatrics and Adolescent Medicine, Medical University of Vienna, 1090 Vienna, Austria, the [t]Department of Genetics, Children's Hospital of Eastern Ontario, Ottawa, Ontario K1H 8L1, Canada, the [u]Yorkshire Regional Genetic Service, Chapel Allerton Hospital, Leeds, West Yorkshire LS9 7TF, United Kingdom, the [v]Neonatal Unit, Bradford Royal Infirmary, Bradford, West Yorkshire BD9 6RJ, United Kingdom, [w]Génétique, Pôle Mère, Enfant, Centre Hospitalier d'Arras, 62 000 Arras, France, [x]Clalit Health Services, Shfaram 20200, Israel, the [y]Zlotowski Center for Neuroscience, Ben-Gurion University of the Negev, Beer-Sheva 8410501, Israel, the [z]Epilepsy Research Centre, Melbourne Brain Centre, Austin Health, Heidelberg 3084, Victoria, Australia, and the [aa]Institut de Pathologie et de Génétique ASBL/IRSPG, B-6041 Gosselies, Belgium

Background: Hyperekplexia mutations have provided much information about glycine receptor structure and function.
Results: We identified and characterized nine new mutations. Dominant mutations resulted in spontaneous activation, whereas recessive mutations precluded surface expression.
Conclusion: These data provide insight into glycine receptor activation mechanisms and surface expression determinants.
Significance: The results enhance our understanding of hyperekplexia pathology and glycine receptor structure-function.

Hyperekplexia is a syndrome of readily provoked startle responses, alongside episodic and generalized hypertonia, that presents within the first month of life. Inhibitory glycine receptors are pentameric ligand-gated ion channels with a definitive and clinically well stratified linkage to hyperekplexia. Most hyperekplexia cases are caused by mutations in the α1 subunit of the human glycine receptor (hGlyR) gene (*GLRA1*). Here we analyzed 68 new unrelated hyperekplexia probands for *GLRA*1 mutations and identified 19 mutations, of which 9 were novel. Electrophysiological analysis demonstrated that the dominant mutations p.Q226E, p.V280M, and p.R414H induced spontaneous channel activity, indicating that this is a recurring mechanism in hGlyR pathophysiology. p.Q226E, at the top of TM1, most likely induced tonic activation via an enhanced electrostatic attraction to p.R271 at the top of TM2, suggesting a structural mechanism for channel activation. Receptors incorporating p.P230S (which is heterozygous with p.R65W) desensitized

* This work was supported by the Australian Research Council (JWL), Waterloo Foundation (MIR), the National Institute of Social Care and Health Research (NISCHR-RRG; to MIR, RHT and SKC), Wales Gene Park (MIR).
[1] Both authors contributed equally to this work.
[2] Supported by an Epilepsy Research UK fellowship.
[3] Supported by the National Health and Medical Research Council. To whom correspondence should be addressed: Queensland Brain Institute, University of Queensland, Brisbane, Queensland 4072, Australia. Tel.: 617-3346-6375; Fax: 617-3346-6301; E-mail: j.lynch@uq.edu.au.

much faster than wild type receptors and represent a new TM1 site capable of modulating desensitization. The recessive mutations p.R72C, p.R218W, p.L291P, p.D388A, and p.E375X precluded cell surface expression unless co-expressed with α1 wild type subunits. The recessive p.E375X mutation resulted in subunit truncation upstream of the TM4 domain. Surprisingly, on the basis of three independent assays, we were able to infer that p.E375X truncated subunits are incorporated into functional hGlyRs together with unmutated α1 or α1 plus β subunits. These aberrant receptors exhibit significantly reduced glycine sensitivity. To our knowledge, this is the first suggestion that subunits lacking TM4 domains might be incorporated into functional pentameric ligand-gated ion channel receptors.

The glycine receptor chloride channel (GlyR),[4] a member of the pentameric ligand-gated ion channel (pLGIC) family, mediates inhibitory neurotransmission in the spinal cord, brain stem, and retina (1). Functional pLGICs comprise of homo- or hetero-pentamers with subunits arranged around a central ion-conducting pore (2). Each subunit contains an extracellular domain harboring the neurotransmitter binding site and a transmembrane domain comprising four transmembrane α-helices (TM1–TM4) connected by flexible loops. A total of five GlyR subunit genes exist in humans (α1–α4 and β), although the α4 (*GLRA4*) locus is considered a pseudo-gene because of a premature stop codon in the TM3-TM4 domain (3). Synaptic GlyRs comprise two α and three β subunits (4, 5), although extrasynaptic homomeric α GlyRs are also found (6). Because the $\alpha1\beta$ GlyR is the sole stoichiometry responsible for inhibitory neurotransmission in motor reflex arcs of the spinal cord (6), mutations impairing the function of either the α1 or β subunit would be expected to impair motor performance.

The evidence for the neuromotor role of the GlyR is provided by the unequivocal link between glycinergic genes and hyperekplexia, a rare neurological disorder (7, 8). Hyperekplexia (also known as startle disease) is characterized by readily provoked startle responses, alongside a generalized and episodic hypertonia that presents within the first month of life. A proportion of cases have an increased likelihood of delay in speech acquisition, intellectual disability, and recurrent neonatal and infantile apneas, which gradually normalize during the first years of life. During development into adulthood, the condition typically evolves into a lifelong predisposition to excessive startle reflexes, triggered by unexpected auditory and tactile stimuli, which then cause startle-induced falls leading to repeated injuries. Hyperekplexia is caused not only by hereditary and *de novo* mutations in the human GlyR α1 and β subunit genes (7, 9–13) but also by mutations in other proteins important for the formation and maintenance of glycinergic synapses (14–16). Mutations in the α1 and β subunits result in changes in the surface expression efficiency or in the functional properties of synaptic $\alpha1\beta$ GlyRs, thereby disrupting inhibitory neurotransmission in motor reflex circuits.

[4] The abbreviations used are: GlyR, glycine receptor; hGlyR, human GlyR; pLGIC, pentameric ligand-gated ion channel; TM, transmembrane; MTSR, sulforhodamine methanethiosulfonate.

We previously presented the results of a sequencing screen of the GlyR α1 subunit (*GLRA1*) in 88 unrelated hyperekplexia probands from where we identified a total of 19 mutations, 12 of which were novel (10). We demonstrated that dominant mutations typically disrupt receptor function without changing their surface expression efficiency, whereas recessive mutations generally preclude functional receptor expression when expressed either as mutated α1 homomers or as heteromers with the β subunit. In the present study, 68 new unrelated patients with a clinical diagnosis of hyperekplexia were screened for mutations in *GLRA1*. The screening revealed a total of 19 mutations, of which 9 were novel. All new mutations were characterized in terms of their electrophysiological properties and their cell surface localization. Additionally, a previously characterized mutation, p.R65W (10), was reinvestigated because of its presumed compound heterozygosity with the new mutation, p.P230S. The subsequent functional investigation of the hyperekplexia mutations revealed three residues critical for GlyR channel opening, providing insight into pLGIC activation mechanisms, and one novel residue playing an important role in desensitization.

EXPERIMENTAL PROCEDURES

Patient Samples—A total of 68 unrelated probands with a clinical diagnosis of hyperekplexia were recruited for this study with appropriate ethical approval and consent procedures in place (South West Wales Regional Ethics Committee). Referral was initiated from neurologists, pediatricians, or clinical geneticists from the United Kingdom and several international centers. Diagnostic criteria for hyperekplexia included a nonhabituating startle response (positive nose tap test), often with neonatal apnea, a history of infantile hypertonicity, and clinical exclusion of phenocopies such as startle epilepsy or early encephalopathy (17, 18).

Molecular Genetics—Multiplex PCR amplification (Qiagen) was employed to rapidly amplify all coding exons and flanking intronic regions of *GLRA1*. Purified PCR amplimers were Sanger sequenced using ABI^{TM} capillary technology (Applied Biosystems, Inc., Foster City, CA). The frequency of variants identified was determined by screening a panel of 100 commercial control samples using restriction fragment length polymorphism if a suitable restriction enzyme was available or by high resolution melt analysis performed on Lightscanner (Idaho Technologies). Detection of large deletions or insertions was performed using multiplex ligation-dependent probe amplification (MRC-Holland) according to the manufacturer's protocol. Additionally, confirmation of the recurrent exon 1–7 deletion mutation was carried out using break point PCR analysis (19). Mutations were introduced into pRK5-hGlyRα1 using the QuikChange site-directed mutagenesis kit (Stratagene) and confirmed by direct sequencing of the entire transgene-coding region (10).

Fluorescence-based Imaging—Experiments were performed on HEK AD293 cells cultured in Dulbecco's modified Eagle's medium supplemented with 10% fetal calf serum and 1% penicillin/streptomycin. The α1 wild type subunit, the β wild type subunit, and the plasmids containing hyperekplexia mutations were all co-transfected in equal amounts. The pcDNA3-YFP-I152L plasmid was co-transfected in an amount equal to the sum

of all transfected GlyR plasmid amounts. When the transfection was terminated 16 h later by rinsing with fresh culture medium, cells were plated into the wells of a 384-well plate. Within the following 24–32 h, the cell culture medium was replaced by an extracellular control solution (140 mM NaCl, 5 mM KCl, 2 mM $CaCl_2$, 1 mM $MgCl_2$, 10 mM HEPES, and 10 mM glucose, pH 7.4). Cells were imaged with an automated fluorescence-based screening system using YFP-I152L fluorescence quench as an indicator of anion influx rate (20). During experiments, fluorescence images of each well were obtained twice: once before and once after the application of a sodium iodide solution (140 mM NaI, 5 mM KCl, 2 mM $CaCl_2$, 1 mM $MgCl_2$, 10 mM HEPES, and 10 mM glucose, pH 7.4) containing defined concentrations of glycine. Mean percentage quench values represent data averaged from four experiments carried out on different plates. Each experimental value was an average of the percentage quench of all fluorescent cells in three wells on the same plate, with each well containing >200 cells. To determine the glycine dose-response curve from these data, an empirical three-parameter Hill equation was fitted by a nonlinear least squares algorithm using SigmaPlot 12.0 software.

Electrophysiology—Glycine-gated currents were measured in HEK AD293 cells transfected as described above. Recordings were performed by whole cell patch clamp electrophysiology at a holding potential of −40 mV. Alternatively, spontaneous single-channel currents were recorded from outside-out excised patches, held at −70 mV in the absence of agonist, except for α1 wild type receptors, which opened too infrequently in glycine-free solution to obtain accurate estimates of current amplitude. Current amplitude for wild type receptors was instead estimated from recordings in the presence of 1 mM glycine. During experiments, cells were continually superfused with the extracellular control solution as detailed above. Patch pipettes were pulled to a final tip resistance of 1–4 MΩ (whole cell) or 6–12 MΩ (outside-out) when filled with a standard intracellular solution (145 mM CsCl, 2 mM $CaCl_2$, 2 mM $MgCl_2$, 10 mM HEPES, and 10 mM EGTA, pH 7.4). Whole cell currents, which were filtered at 1 kHz and digitized at 2 kHz, were recorded using an Axon MultiClamp 700B amplifier (Molecular Devices). Single-channel currents, filtered at 5 kHz and digitized at 20 kHz, were recorded using an Axon Axopatch 200B amplifier (Molecular Devices). Voltage clamp fluorometry experiments were performed as previously described (21). Briefly, oocytes were removed from the ovaries of *Xenopus laevis* frogs, incubated in OR-2 (82.5 mM NaCl, 2 mM KCl, 1 mM $MgCl_2$, and 5 mM HEPES, pH 7.4) containing 1.5 mg/ml collagenase for 2 h at room temperature on a shaker and co-injected with 5 ng of pGEMHE-hGlyRα1 and 25 ng of pGEMHE-hGlyRα1-R271C/E375X RNA into the cytosol. Oocytes were cultured for 2–3 days at 18 °C in ND96 (96 mM NaCl, 2 mM KCl, 1 mM $MgCl_2$, 1.8 mM $CaCl_2$, and 5 mM HEPES, pH 7.4) containing 275 mg/liter sodium pyruvate, 110 mg/liter theophylline, and 0.1% (v/v) gentamicin. For labeling, oocytes were incubated with 10 μM sulforhodamine methanethiosulfonate (MTSR) diluted in ND96 for 1 min on ice. 3 mM KCl was used as internal solution, and recordings were performed at −40 mV.

Immunofluorescence—GlyR α1 subunits were transiently expressed in HEK293 cells using the Magnetofection™ method (Oz Biosciences). Around 24 h post-transfection, cells were fixed in 4% (w/v) paraformaldehyde for 5 min at room temperature. Cells were quenched with 50 mM NH_4Cl in PBS. Fixed cells were permeabilized with PBS containing 0.1% (v/v) Triton X-100 (Sigma), 10% (v/v) fetal calf serum (Sigma), and 0.5% (w/v) bovine serum albumin (fraction V; Sigma) to allow for intracellular immunostaining. Receptor sublocalization was determined using rabbit monoclonal anti-GlyR α1 (1:400; Millipore) primary antibody and with goat anti-rabbit secondary antibody, conjugated with Alexa Fluor 488 (1:200; Invitrogen). Cell surface immunostaining was conducted using the same reagents, antibodies, and dilutions but carried out prior to paraformaldehyde fixation. Fixed cells were then quenched with 50 mM NH_4Cl before mounting on glass slides. Cell images were acquired using a Zeiss LSM 710 confocal microscope with ZEN software. The master gain was kept constant to compare the expression of α1 GlyR mutants relative to wild type. Transfection was repeated three times.

Molecular Modeling—Wild type and mutated forms of the human α1 GlyR were modeled by 50% homology (69% sequence coverage) with Protein Data Bank structure 3RHW, the glutamate-gated chloride channel receptor (α GluClR) from *Caenorhabditis elegans* (22). Using our multitemplate homology modeling pipeline, this was one of three Protein Data Bank homologues that were identified and used in the assembly of the α1 GlyR models, 3RHW (chain E), 1VRY (chain A), and 1MOT (chain A). The homology modeling pipeline was built with the Biskit structural bioinformatics platform (23). Our pipeline workflow incorporates the NCBI tools platform (24), including the BLAST program for similarity searching of sequence databases. T-COFFEE (25) was used for alignment of the test sequence with the template, followed by iterations of the MODELLER-9.11 program (26) to generate the final model structure. The Chimera program (27) was used for the viewing of models and generation of images.

RESULTS

Mutation Analysis—A total of 68 probands with hyperekplexia were assessed for genetic variation in *GLRA1* coding regions. All sequence variations were cross-referenced with the dbSNP database and our previous *GLRA1* data sets (for recurrent mutations) and were regarded as probable mutations following exclusion from a panel of 100 control samples and the exome variants server. The screening revealed 19 mutations in 21 hyperekplexia probands (Table 1), a rate that is consistent with previous studies (10, 28). Nine mutations were novel in the public domain, and three (one novel and two recurrent) mutations were present in more than one individual. Note that p.R414H has since been reported as a very rare variant in dbSNP (rs200130685), with a heterozygosity of 0.002 and a minor allele frequency of 0.0233 from the exome variants server. Consistent with previous studies, deletion and nonsense mutations were associated with recessive inheritance (homozygous or compound heterozygous), whereas missense mutations resulted in a dominant or recessive effect depending on their position in the polypeptide. The majority of index cases showed recessive inheritance (15 of 21; 71%), including cases 12 and 19 with confirmed compound heterozygosity as mutations were

TABLE I
Details of hyperekplexia mutations identified in this study

Case	Genotype	Inheritance mode	Class of mutation	Protein mutation			Protein position	Gender	Reference
1 - 4	Exons 1-7	recessive	deletion	delEX1-7			N-terminal-M2	2x male, 2x female	(29)
5	C573T	compound heterozygote	missense	p.R65W	}	unknown	N-terminal	male	(10)
	C1068T		missense	p.P230S		unknown	M1		novel
6 - 7	C594T	recessive	missense	p.R72C			N-terminal	2x female	novel
8	C1032T	recessive	missense	p.R218W			N-terminal	male	novel
9	G687A	recessive	missense	p.E103K			N-terminal	male	(10)
10	C971A	recessive	nonsense	p.Y197X			N-terminal	male	(10)
11	C986A	recessive	nonsense	p.Y202X			N-terminal	male	(28)
12	G1033A	compound heterozygote	missense	p.R218Q	}	paternal	N-terminal	male	(51)
	C1267A		nonsense	p.S296X		maternal	M3		(52)
13	C1056G	dominant	missense	p.Q226E			M1	male	novel
14	G1135A	recessive	missense	p.R252H			M1-M2		(53)
15 - 16	G1192A	dominant	missense	p.R271Q			M2-M3	2x female	(54)
17	A1216G	dominant	missense	p.Y279C			M2-M3	female	(55)
18	G1218A	dominant	missense	p.V280M			M2-M3	male	novel
19	T1252C	compound heterozygote	missense	p.L291P	}	paternal	M3	female	novel
	A1543C		missense	p.D388A		maternal	M3-M4		novel
20	G1503T	recessive	nonsense	p.E375X			M3-M4	male	novel
21	G1621A	dominant	missense	p.R414H			C-terminal	male	rs200130685*

* p.R414H was a novel variant at the time of identification but since it is listed as a very rare variant in dbSNP.

segregated back to parental DNA. It is likely that sample 5 represents a third case of compound heterozygosity; however, parental DNA was not available for confirmation. Four index cases of Turkish origin displayed a recessive homozygous deletion of exons 1–7, further confirming this deletion as a significant population-specific risk allele (10, 29). Dominant mutations were mainly located in the discrete transmembrane α-helices, whereas recessive mutations were spread throughout the protein. Phylogenetic alignment of all novel missense mutations established that they altered conserved amino acids and were protein-damaging when assessed using the Sorting Intolerant from Tolerant (SIFT) tool (accessible online). The functional impact of the novel mutations was further investigated under recombinant conditions that simulated the dominant, recessive, and compound heterozygous inheritance modes.

Functional High Throughput Analysis—The first round of functional characterization involved imaging live transfected cells via an automated fluorescence-based screening system using YFP-I152L fluorescence quench as an indicator of anion influx rate (20). The advantage of this approach over electro-

physiology is that responses of large cell numbers can be averaged, thus permitting the reliable quantitation of small changes in the functional expression levels of mutated GlyR isoforms. To investigate the functional properties of the mutated receptors, HEK AD293 cells were transiently transfected with wild type and mutated subunits in various combinations in an attempt to simulate dominant, recessive, and compound heterozygous inheritance modes. Each mutated subunit was expressed on its own, with the β wild type subunit, with the α1 wild type subunit, and with both α1 and β wild type subunits together. These experiments are summarized as: 1) mutant alone, 2) mutant + β, 3) mutant + α1, and 4) mutant + α1β. For compound heterozygous mutations, the mutated subunits were also co-transfected together with and without the β wild type subunit, *i.e.*, 5) first mutant + second mutant and 6) first mutant + second mutant + β. Fluorescent cells were considered as expressing functional GlyRs when the quench was a least 10% greater than the quench from cells expressing YFP only (no receptors).

Glycine dose-response experiments showed that the glycine sensitivity was reduced for all recessive and compound heterozygous mutations relative to α1 wild type GlyRs (Fig. 1*A*). With the exception of the p.P230S mutation, which expressed as a homomer, the recessive and compound heterozygous mutated subunits only showed a response to glycine if the α1 wild type subunit was co-expressed. Note that co-expression of these mutated α1 subunits with the β wild type subunit did not produce functional expression. Receptors incorporating both compound heterozygous mutations, p.L291P and p.D388A, showed no evidence of glycine sensitivity regardless of the presence of the β subunit. In contrast, receptors incorporating both p.R65W and p.P230S responded to glycine with and without β subunit co-expression, albeit with dramatically reduced glycine sensitivity. Because the glycine sensitivity was decreased for all mutated subunits when co-expressed with the α1 wild type subunit, we concluded that all recessive and compound heterozygous mutated subunits were incorporated into functional GlyRs as heteromers, if not as homomers.

For the three novel dominant mutations, in the case of p.R414H, no significant change in glycine EC_{50} was detected (Fig. 1*A*), and for receptors containing the dominant mutations p.Q226E and p.V280M, the glycine sensitivity could not be determined because fluorescence quench was complete in the absence of glycine. To test whether these three mutations formed spontaneously active channels, we initially bathed cells in NaCl solution and then introduced a high concentration of NaI solution containing no glycine. The results of this experiment, summarized in Fig. 1*B*, show that receptors containing p.Q226E, p.V280M, or p.R414H subunits displayed significant quench in the absence of glycine. Because iodide is highly permeant through GlyRs and quenches YFP-I152L fluorescence much more potently than chloride does, this result provides evidence that these three mutations result in spontaneously active or "leaky" channels. Indeed, the high level of spontaneous activity was the reason why the glycine sensitivity of receptors incorporating p.Q226E and p.V280M mutations could not be quantitated (Fig. 1*A*).

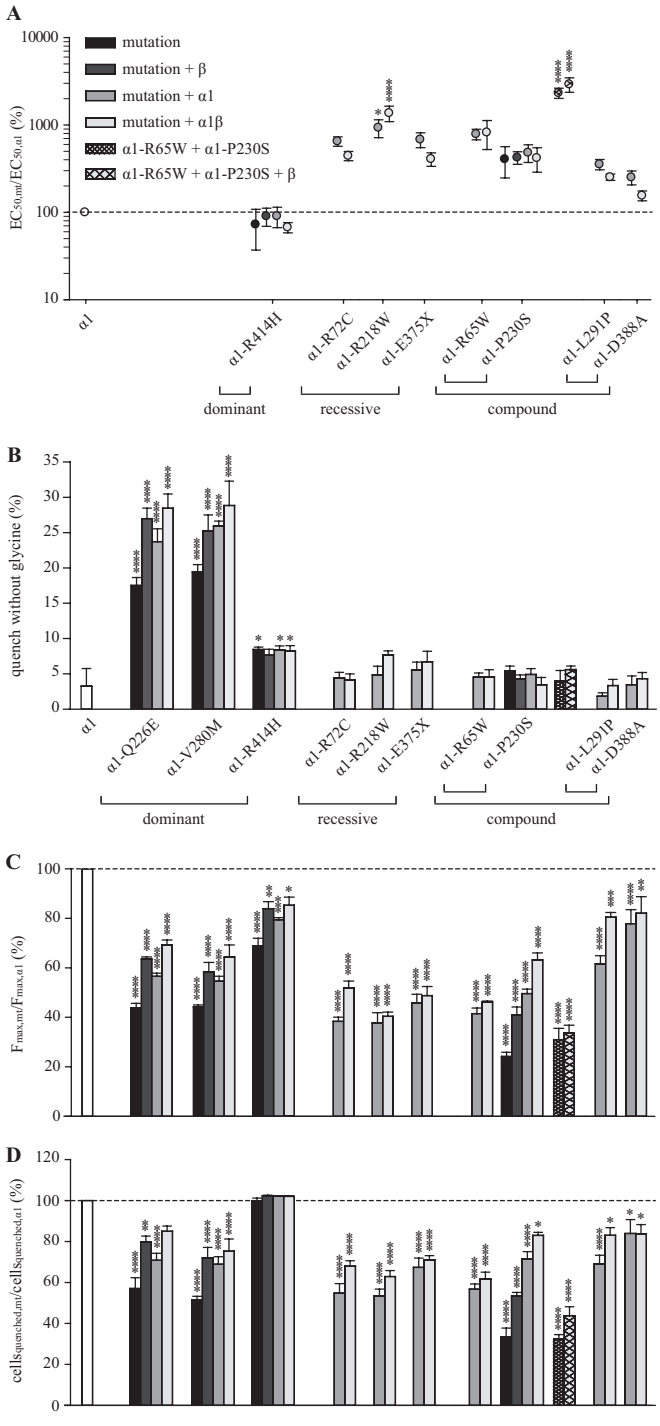

FIGURE 1. **Functional characterization of novel mutations using fluorescence-based imaging.** *A*, normalized glycine EC_{50} values for receptors comprised of the indicated subunit combinations. Results for p.Q226E and p.V280M containing GlyRs are not shown because complete quench occurred in the absence of glycine. For all other mutated receptors, the absence of a plotted result means that the indicated subunit(s) did not express. *B*, mean percentage fluorescence quench observed when NaCl solution was replaced by NaI solution (without glycine). *C*, normalized maximal changes in fluorescence observed upon the addition of NaI containing saturating glycine. The maximal change in fluorescence is presented as the final (quenched) fluorescence value minus the initial fluorescence value. *D*, mean number of quenched cells expressed as a percentage of the total number of fluorescent cells. In *A*, *C*, and *D*, all mutant values were normalized relative to the wild type value obtained from the same plate. In all panels, *p* values were calculated relative to the α1 GlyR using one-way analysis of variance followed by Dunnett's post hoc test: *, $p < 0.05$; **, $p < 0.01$; ***, $p < 0.001$; and ****, $p < 0.0001$.

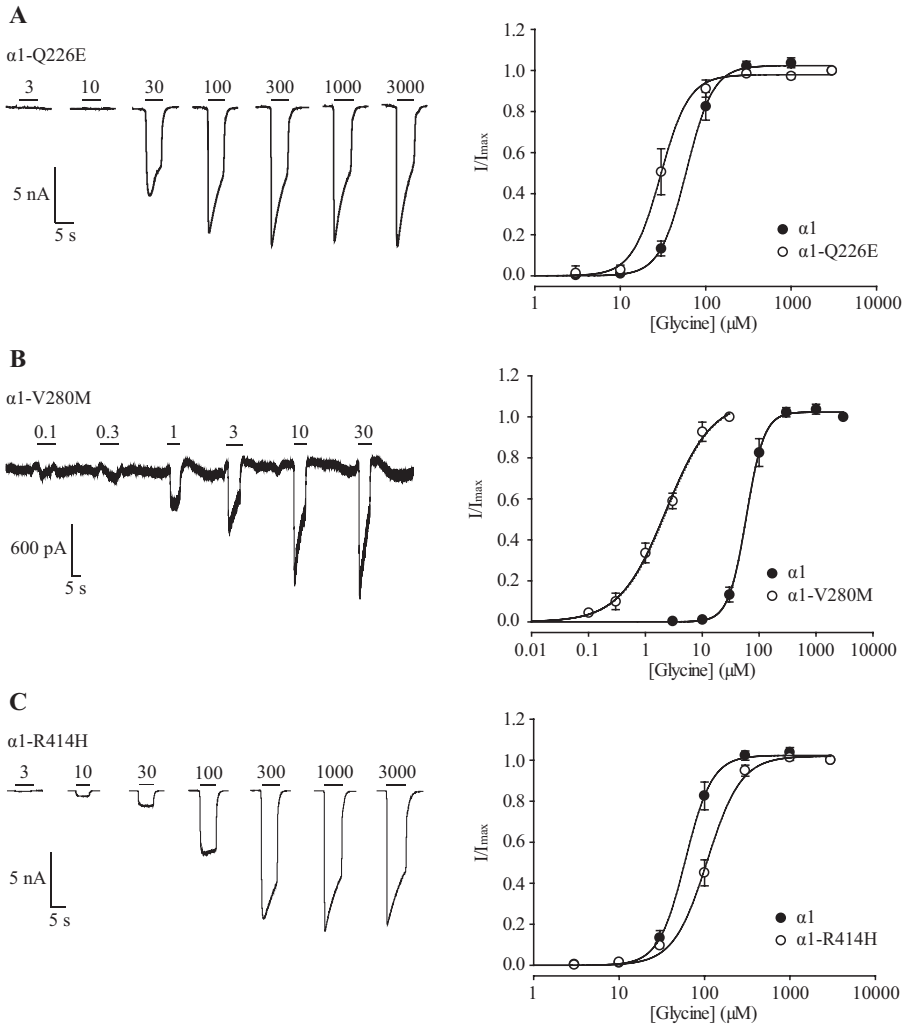

FIGURE 2. **Functional characterization of autosomal dominant mutations by whole cell patch clamp recording.** *A*, sample whole cell current recording for homomeric p.Q226E GlyRs. In this and all subsequent figures, *horizontal bars* indicate the duration of the glycine applications with concentrations shown in μM. The *right panel* represents averaged whole cell glycine dose-response curve for the p.Q226E GlyR. The α1 GlyR dose-response curve plotted here is replicated in all panels displaying dose-response curves in this and subsequent figures. *B*, sample whole cell current recording and averaged whole cell glycine dose-response curve for the homomeric p.V280M GlyR. *C*, sample whole cell current recording and averaged whole cell glycine dose-response curve for the homomeric p.R414H GlyR. Averaged parameters of best fit to all individual dose-response relationships are summarized in Table 2.

In addition, for all functional channels, the anion influx rate was significantly reduced relative to α1 wild type receptors as indicated by their reduced maximal glycine-induced fluorescence quench magnitude (Fig. 1*C*). As noted above, the fluorescence quench for p.Q226E- and p.V280M-containing GlyRs was already maximal in the absence of glycine. Moreover, the percentage of quenched cells relative to the total number of fluorescent cells was significantly reduced for all functional channels relative to α1 wild type receptors (except for p.R414H), suggesting that fewer functional receptors are located at the cell surface (Fig. 1*D*). This observation suggests that the mutations tend to impair functional receptor expression.

Spontaneous Activity as a Mechanism for Dominant Hyperekplexia Mutations—We then employed patch clamp electrophysiology to analyze the effects of the mutations on receptor function at greater precision. Examples of currents activated by increasing glycine concentrations at homomeric α1 GlyRs together with the averaged glycine dose-response relationship are shown in Fig. 2. The mean glycine EC_{50} value of p.Q226E indicates that the glycine sensitivity was not significantly altered (Fig. 2*A* and Table 2). In contrast, for receptors incorporating the dominant mutation p.V280M, the sensitivity to glycine was dramatically increased relative to wild type receptors (Fig. 2*B* and Table 2). The mean glycine EC_{50} value of p.R414H was modestly increased (Fig. 2*C* and Table 2). These results are broadly consistent with the fluorescence data shown in Fig. 1.

For the three novel dominant mutations, our fluorescence assay predicted spontaneous activity for p.Q226E, p.V280M, and p.R414H receptors (Fig. 1*B*), which was then further investigated by recording single-channel activity in outside-out membrane patches bathed in glycine-free extracellular solution. Recordings revealed spontaneous activity for all three mutated homomeric receptors, whereas little, if any, spontaneous activity was ever observed for wild type α1 GlyRs (Fig. 3*A*) consistent with previous reports (30). At a membrane potential of −80 mV, the single-channel current amplitude for p.Q226E

TABLE 2
Properties of novel mutations using whole cell patch clamp electrophysiology

	EC_{50}	n_H	I_{max}	n
	μM		nA	
Wild type				
$\alpha 1$	64 ± 8	3.8 ± 0.3	19 ± 3	10
$\alpha 1\beta$	39 ± 4	2.4 ± 0.2	14 ± 3	5
Dominant mutations				
p.Q226E	32 ± 6	3.5 ± 0.7	10 ± 5	3
p.V280M	2.4 ± 0.3	1.1 ± 0.2[b]	5 ± 4[d]	3
p.R414H	110 ± 12	2.3 ± 0.2[c]	13 ± 1	4
Recessive mutations				
p.R72C + $\alpha 1$	189 ± 14	2.9 ± 0.1	8 ± 3[c]	4
p.R218W + $\alpha 1$	235 ± 26	2.4 ± 0.2	6 ± 2[d]	4
p.E375X + $\alpha 1$	243 ± 20	1.8 ± 0.2[d]	1.2 ± 0.4[a]	4
p.E375X + $\alpha 1\beta$	140 ± 22	2.2 ± 0.2	9 ± 4	3
Compound heterozygous mutations				
p.R65W + $\alpha 1$	1468 ± 557[a]	1.0 ± 0.1[a]	2.9 ± 1.3[a]	6
p.R65W + $\alpha 1\beta$	1281 ± 315[a]	1.1 ± 0.2[d]	1.2 ± 0.9[b]	5
p.P230S	172 ± 50	1.6 ± 0.1[a]	1.6 ± 0.5[a]	6
p.P230S + β	155 ± 26	2.4 ± 0.3	2.2 ± 1.0[b]	6
p.L291P + $\alpha 1$	198 ± 15	3.1 ± 0.5	9 ± 1[c]	5
p.L291P + $\alpha 1\beta$	180 ± 22	2.2 ± 0.3	7 ± 1	4
p.D388A + $\alpha 1$	173 ± 11	2.8 ± 0.7	6 ± 2[d]	5
p.D388A + $\alpha 1\beta$	170 ± 16	2 ± 0.2	9 ± 3	4

[a] $p < 0.0001$ relative to the corresponding homo- or heteromeric wild type GlyR via one-way ANOVA followed by Dunnett's post hoc test.
[b] $p < 0.001$ relative to the corresponding homo- or heteromeric wild type GlyR via one-way ANOVA followed by Dunnett's post hoc test.
[c] $p < 0.05$ relative to the corresponding homo- or heteromeric wild type GlyR via one-way ANOVA followed by Dunnett's post hoc test.
[d] $p < 0.01$ relative to the corresponding homo- or heteromeric wild type GlyR via one-way ANOVA followed by Dunnett's post hoc test.

receptors was smaller (4.5 ± 0.1 pA, $n = 4$ patches; Fig. 3*B*) than for wild type $\alpha 1$ receptors (7.2 ± 0.1 pA, $n = 3$; Fig. 3*A*), whereas the amplitude for p.V280M receptors was unchanged (7.1 ± 0.2 pA, $n = 3$; Fig. 3*C*), and the magnitude of p.R414H receptors was larger (8.4 ± 0.2 pA, $n = 3$; Fig. 3*D*). The corresponding conductance values at −80 mV, a Cl^- equilibrium potential of 0 mV, and a liquid junction potential of 4 mV, were 97.3, 60.8, 95.9, and 110.8 pS for wild type, p.Q266E, p.V280M, and p.R414H receptors, respectively. Applying a saturating concentration of glycine, measuring the peak current response, and dividing that by the single-channel amplitude provided an estimate of the minimum number of channels contained in each recorded patch. Open probability (P_o) was determined using segments of record that contained no evidence of multiple, superimposed openings. A total of 5–6 min of recording was selected across three or four patches for each channel type. Estimated P_o values determined in this way should be regarded as upper limits and were as follows: p.Q226E, 0.03; p.V280M, 0.07; and p.R414H, <0.001. Wild type homomeric receptors opened too infrequently in glycine-free solution to obtain a reliable P_o measurement. It was, however, dramatically reduced relative to the mutated GlyRs.

Incorporation of TM4 Truncated Subunits—Subunits incorporating the recessive mutation p.R72C, p.R218W, or p.E375X were only functional when co-expressed with the $\alpha 1$ wild type subunit. The glycine sensitivities and the maximal current amplitudes of receptors incorporating these mutations were reduced relative to those of wild type receptors (Fig. 4, *A–D*, and Table 2) in agreement with the results from the fluorescence assay (Fig. 1). For all $\alpha 1\beta$ heteromeric receptors, β subunit incorporation was confirmed pharmacologically by its characteristic reduction in sensitivity to lindane inhibition (31) For example, in Fig. 4*D* (*lower panel*), we confirmed that $\alpha 1$ wild type GlyRs are strongly inhibited by 100 μM lindane, whereas $\alpha 1\beta$ wild type GlyRs are resistant. Because receptors formed by co-expression of p.E375X, $\alpha 1$ wild type, and β wild type subunits were also resistant to lindane and showed decreased glycine sensitivity relative to $\alpha 1\beta$ GlyRs (Fig. 4*D* and Table 2), we infer that p.E375X subunits were incorporated into functional $\alpha 1\beta$ heteromeric GlyRs.

We were surprised to observe that the truncation mutation, p.E375X, which has lost the TM4 domain, reduced the glycine sensitivity significantly ($p < 0.001$ relative to $\alpha 1$ wild type via unpaired *t* test) when co-expressed with the $\alpha 1$ wild type subunit (Fig. 4, *C* and *D*). The reduced glycine sensitivity was only partly compensated by co-expressing the β wild type subunit. This result strongly suggests that the truncated subunit is incorporated into functional receptors, which is unexpected given that previous GlyR studies indicated that TM4 deletion is incompatible with the surface expression of functional $\alpha 1$ GlyRs (32–35). Given our unexpected result, we sought to confirm whether the p.E375X mutant subunit was incorporated into functional GlyRs using voltage clamp fluorometry.

Voltage clamp fluorometry involves introducing a cysteine into a receptor domain of interest and covalently tagging it with a sulfhydryl-labeled fluorophore, commonly a rhodamine derivative such as MTSR. Because the quantum efficiency of rhodamine fluorescence is proportional to the hydrophobicity of its environment, a glycine-induced fluorescence change can be interpreted as a local conformational change at the labeled site (36). Voltage clamp fluorometry is thus able to report conformational rearrangements in real time at defined locations on the surface of the labeled subunit. These experiments were performed on receptors expressed in *Xenopus* oocytes as HEK293 cells exhibit an unacceptably high level of nonspecific MTSR labeling. The MTSR-labeled p.R271C mutant $\alpha 1$ GlyR produces a fluorescence change of ~20% upon activation with 10 mM (saturating) glycine (21). When the p.E375X truncation subunit, also labeled at p.R271C, was expressed together with the $\alpha 1$ wild type subunit, the activation of the recombinant

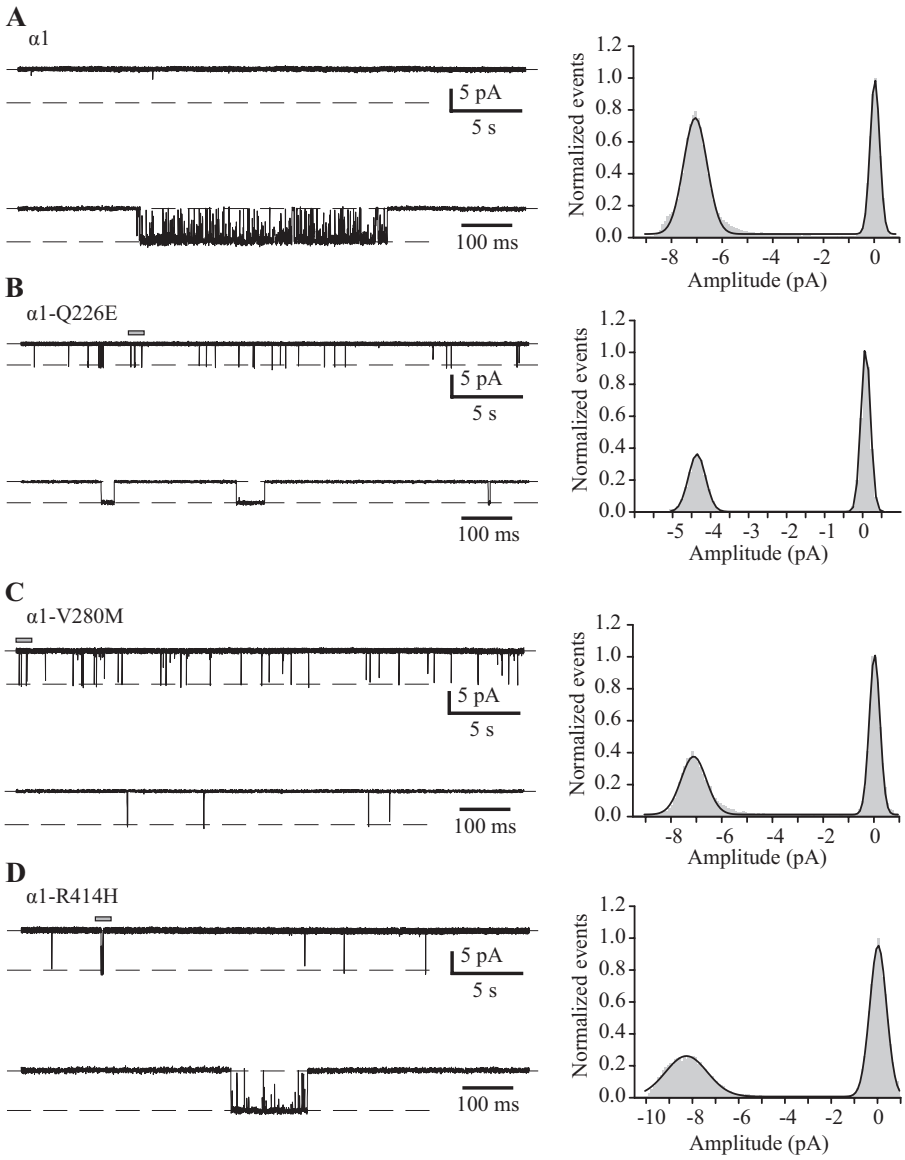

FIGURE 3. **Single-channel recordings of homomeric α1 wild type and spontaneously open mutant GlyRs.** *A*, single-channel current recording of a patch expressing wild type receptors in the absence of glycine. Because of its low open probability in glycine-free solution, the higher resolution recording and accompanying amplitude histogram was obtained in 1 mM glycine. *B*, a sample recording of spontaneous single-channel activity in an outside-out patch expressing p.Q226E, along with the amplitude histogram for the same patch. *C*, a sample single-channel recording from a patch expressing p.V280M receptors, along with the amplitude histogram for the same patch. *D*, a sample single-channel recording from a patch expressing p.R414H receptors, along with the amplitude histogram for the same patch. Channel openings are represented by downward deflections with the mean open current level indicated by *dashed lines*. The recordings in *B–D* were made in glycine-free solution. For these recordings, the activity *above* the *horizontal bar* in the lower resolution segment is reproduced at higher resolution *below*. Mean channel conductances and open probabilities are given in the text.

receptors by saturating (10 mM) glycine generated currents with a mean maximal current amplitude of 4.8 ± 0.5 μA and a maximal change in fluorescence of 0.7 ± 0.1% (n = 4; Fig. 4*E*). Control current and fluorescence traces from an MTSR-labeled p.R271C mutant GlyR are also shown. In contrast, unlabeled GlyRs comprising the same subunits yielded no significant glycine-induced fluorescence change (data not shown). This provides strong evidence for the surface expression of p.E375X subunits and also suggests that they experience a conformational change upon glycine-induced receptor activation. Because the fluorescence change we observed is smaller than the change in fluorescence for homomeric p.R271C mutant α1 GlyRs (21), we infer that the p.E375X subunit is either incorporated into functional receptors at a low rate or that its conformational change is different from that of full-length p.R271C α1 GlyRs.

Functional Effects in Heterozygous State—Receptors incorporating the compound heterozygous mutation p.R65W showed drastically decreased glycine sensitivity and decreased maximal current amplitudes independent of β subunit expression (Fig. 5*A* and Table 2). The p.P230S mutation also decreased glycine sensitivity and maximal current amplitudes in the presence and absence of the β subunit (Fig. 5*B* and Table 2). All electrophysiological results for the p.R65W and p.P230S mutations are consistent with the fluorescence data described above (Fig. 1). It is also evident in Fig. 5*B* that p.P230S induces fast desensitization. These receptors exhibited a mean decay time constant of 0.9 ± 0.3 s for 3 mM glycine (*cf.* wild type

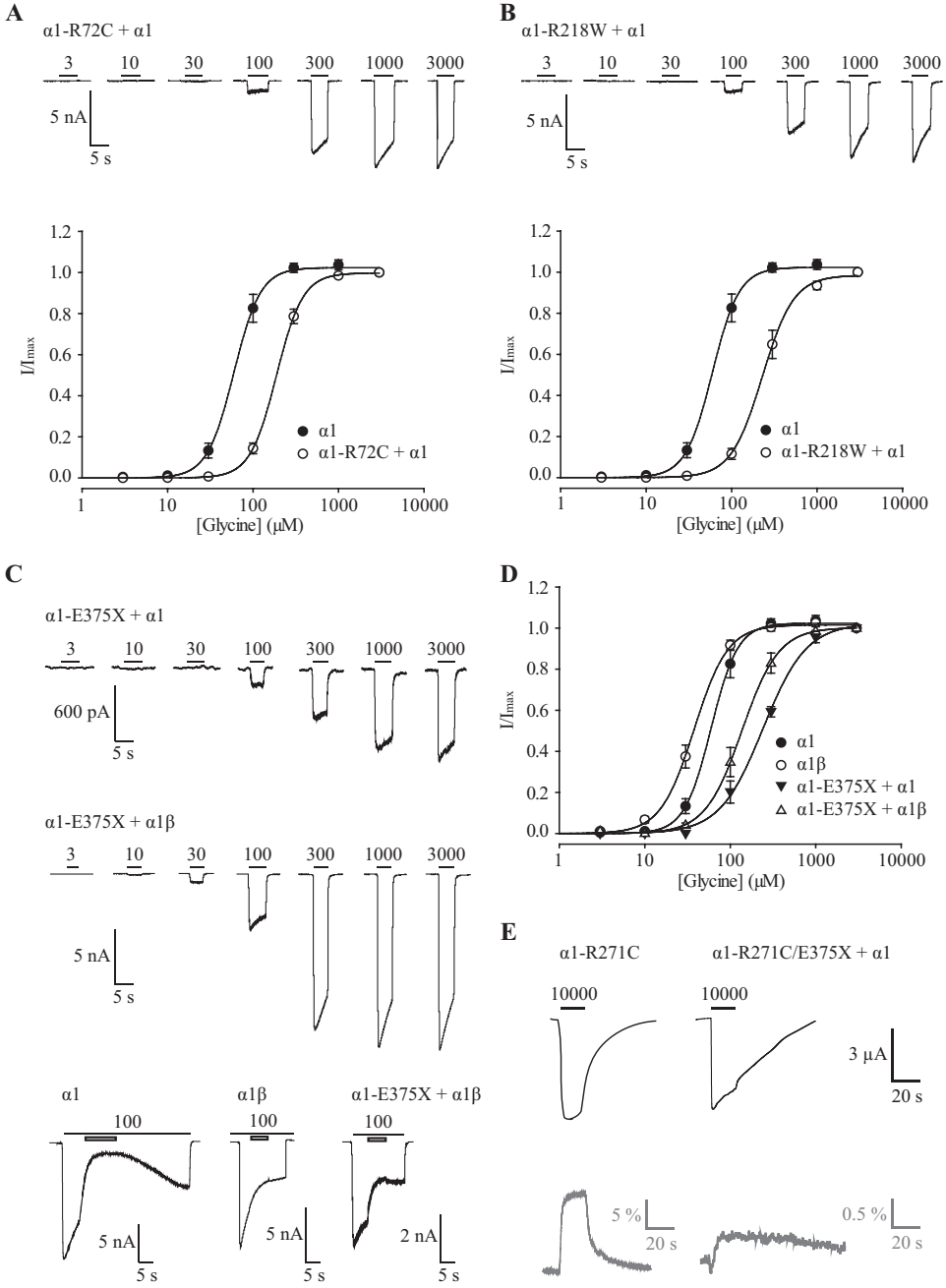

FIGURE 4. **Functional characterization of autosomal recessive mutations by whole cell patch clamp recording and voltage clamp fluorometry.** *A*, sample glycine dose-response trace for p.R72C GlyRs co-expressed with the α1 wild type subunit and normalized glycine dose-response relationship. *B*, sample glycine dose-response trace for p.R218W GlyRs co-expressed with the α1 wild type subunit and normalized glycine dose-response relationship. *C*, sample glycine dose-response traces for p.E375X GlyRs expressed together with α1 wild type or α1 wild type plus β wild type subunits as indicated. For this and all subsequent current recordings, *unfilled bars* represent the application of 100 μM lindane. The lack of lindane inhibition indicates strong expression of β subunits. The α1β GlyR dose-response curve plotted here is replicated in all dose-response curve panels in Fig. 5. The *bottom panel* shows evidence for the efficient incorporation of β subunits into functional GlyRs. α1 homomeric GlyRs are strongly inhibited by 100 μM lindane (*left trace*), whereas α1β GlyRs are resistant (*center trace*). The *right trace*, recorded from the same cell as represented above in *C*, shows that channels formed by the co-expression of p.E375X, α1 and β wild type subunits are also resistant to lindane. Using an unpaired *t* test, mean lindane inhibition of these mutated receptors was significantly different to α1 ($p < 0.001$) but not to α1β receptors ($p = 0.393$). *D*, normalized glycine dose-response curves for α1 homomeric and α1β heteromeric receptors incorporating p.E375X. Averaged parameters of best fit to all individual dose-response relationships are summarized in Table 2. *E*, sample current (*black*) and fluorescence (*gray*) responses induced by the application of 10 mM glycine in receptors comprising p.R271C/E375X and α1 wild type subunits and labeled with MTSR. Averaged results are summarized in the text. Control recordings from MTSR-labeled p.R271C GlyRs are also shown.

receptors: 7.2 ± 1.7 s). Receptors containing the compound heterozygous mutations p.L291P or p.D388A were only functional when each mutated α1 subunit was co-expressed with the α1 wild type subunit (Fig. 1). Electrophysiological recordings revealed that the p.L291P mutation decreased glycine sensitivity but not maximal current amplitudes (Fig. 5*C* and Table 2). The p.D388A mutation decreased glycine sensitivity and maximal current amplitudes (Fig. 5*D* and Table 2). For both mutations, the changes relative to wild type receptors were independent of β subunit expression.

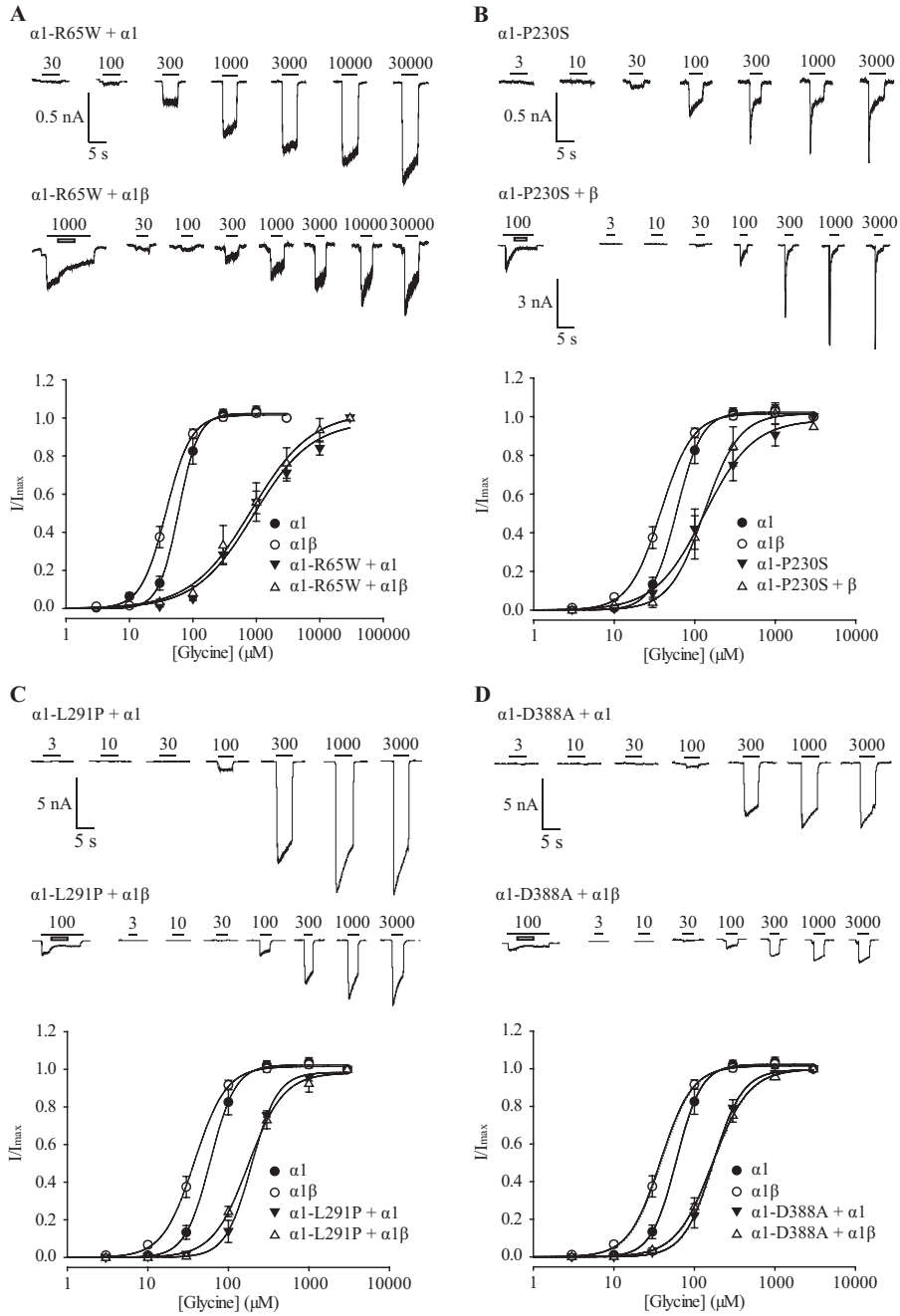

FIGURE 5. **Functional characterization of compound heterozygous mutations by whole cell patch clamp recording.** *A*, sample glycine dose-response traces for p.R65W GlyRs expressed together with α1 wild type or α1 wild type plus β wild type subunits as indicated. Normalized glycine dose-response curves for receptors incorporating p.R65W subunits are shown below. *B*, sample glycine dose-response traces for p.P230S GlyRs expressed either alone or with the β wild type subunit. Normalized glycine dose-response curves for receptors incorporating p.P230S subunits are shown below. *C*, sample glycine dose-response traces for p.L291P GlyRs expressed together with α1 wild type or α1 wild type plus β wild type subunits as indicated. Normalized glycine dose-response curves for receptors incorporating p.L291P are shown below. *D*, sample glycine dose-response traces for p.D388A GlyRs expressed together with α1 wild type or α1 wild type plus β wild type subunits as indicated. Normalized glycine dose-response curves for receptors incorporating p.D388A subunits are shown below. Averaged parameters of best fit to all individual dose-response relationships are summarized in Table 2.

Again, these results are consistent with the fluorescence data presented in Fig. 1.

Cell Surface Localization—Confocal microscopy of transfected cells immunostained with an α1 GlyR antibody was performed to analyze subcellular localization of wild type and mutated receptors. Permeabilized cells were used to determine the intracellular sublocalization of receptors with all constructs showing comparable intracellular expression (Fig. 6, *left panel* of each image pair). Cell surface expression was visualized in nonpermeabilized cells. Cells transfected with wild type and the dominant mutations p.V280M and p.R414H showed immunoreactivity around the cellular circumference indicating localization at the surface (Fig. 6, *right panels*), suggesting that these variants do not affect integration of GlyRs into the cell membrane. The p.Q226E dominant mutation showed reduced immunoreactivity at the cell surface, suggesting that it may

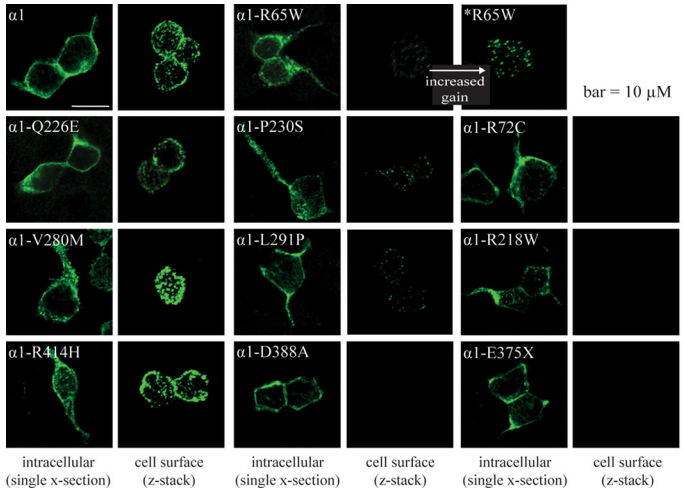

	intracellular	cell surface
α1	+	++
α1-Q226E	+	+
α1-V280M	+	++
α1-R414H	+	++
α1-R65W	+	+
α1-P230S	+	+
α1-L291P	+	+
α1-D388A	+	-
α1-R72C	+	-
α1-R218W	+	-
α1-E375X	+	-

FIGURE 6. **Expression of novel mutations using immunofluorescence.** Images for intracellular expression (*left panels*) were taken as single cross-sectional confocal images and images for cell surface expression (*right panels*) as z-stack images. ++ indicates a high level of cell surface expression comparable with wild type, + indicates a reduction in cell surface expression in comparison to wild type (which was particularly dramatic in the case of p.R65W), and − indicates no visible expression. **R65W* indicates with increased master gain.

impair integration into the surface membrane, unlike the other dominant mutations. The cell surface expression levels of recessive mutated receptors observed in this study showed partial or complete loss of cell surface accumulation. The recessive mutations p.R65W, p.P230S, and p.L291P showed decreased integration into the surface membrane with only partial punctate staining, whereas p.R72C, p.R218W, p.D388A, and p.E375X were completely absent from the cell membrane displaying only cytoplasmic staining (Fig. 6, *right panels*). Surface accumulation of α1 subunits containing these mutations was not detectable with any of the three transfection procedures.

Molecular Modeling—A homology model based on the *C. elegans* glutamate-gated chloride channel receptor crystal structure was used to determine structural mechanisms by which novel mutations disrupted GlyR structure and function (Fig. 7). In particular, the spontaneously active channel p.Q226E affected the TM1 domain toward its extracellular end (Fig. 7, *A* and *B*). Structural modeling showed extension of the TM2 and TM3 helices at their extracellular end, along with extension of the TM4 helix at its intracellular end. Given that p.Q226E faces across the subunit interface toward p.R271 of the adjacent subunit (not shown), an enhanced electrostatic attraction between these two residues may be responsible for the tonic activity induced by p.Q226E. The other spontaneous opener p.V280M affected the extracellular loop between the TM2 and TM3 domain (Fig. 7*C*). This mutation was also found to introduce a kink at the extracellular end of the TM1 helix, perhaps via an altered energetic or steric interaction with I225 across the subunit interface. Also, the TM2 helix was extended at its extracellular end, whereas the TM4 helix was extended at its intracellular end, along with a conformational change at this site. We also observed changes to the conformation of the extracellular domain. In the p.V280M receptor, the α-helix that is found in the wild type subunit between Asp-12 and Arg-20 was lost, and a short helix was introduced around position 72, which would explain its dramatically altered glycine sensitivity. p.R414H affected the C-terminal region at the extracellular end of the TM4 domain, causing profound loss of helical conformation at the cytoplasmic end of the TM4 domain and extension of the TM2 helix at its extracellular end (Fig. 7*D*). Structural modeling suggested that the truncation mutation p.E375X, which lacks the TM4 domain, caused major conformational changes in the TM2 helix via extension of the TM2 helix at its extracellular end and loss of the short helix at the top of the extracellular domain (Fig. 7*E*). The fast desensitizer p.P230S affected the TM1 domain, directly causing a major conformational change by introducing a profound kink at the extracellular end (Fig. 7*F*). In addition, a major conformational change at the cytoplasmic end of the TM3 helix was detected, producing another kink and substantial changes to the TM4 helix. Conformational changes in the extracellular domain included loss of the short helix at the top and β sheet compression.

The impact of the novel dominant mutations upon the pore radius is shown in Fig. 7*G*. For the spontaneously active receptors p.Q226E and p.V280M, channel widening of 1.3 and 4.3 Å, respectively, at the cytoplasmic exit was detected relative to wild type receptors, which is consistent with the observations of a leaky channel. In contrast, the mutation p.R414H had no effect on the pore diameter at the cytoplasmic exit but demonstrates substantial widening toward the extracellular entry, explaining the observed spontaneous channel openings.

DISCUSSION

This study has identified a further 21 *GLRA1*-positive hyperekplexia probands (Table 1) with 19 mutations, of which nine were novel, adding to the compendium of *GLRA1* mutations. Consistent with previous studies (10, 37–40), dominant mutations were expressed at the cell surface, thereby causing changes to the glycine sensitivity, conductance, and/or open probability. In contrast, recessive and compound heterozygous mutations mainly affected cell surface trafficking and insertion of receptors into the membrane (10, 41–43). The mechanisms by which each novel mutation caused hyperekplexia will now be considered in detail.

Genetic screening identified three novel autosomal dominant mutations, p.Q226E, p.V280M, and p.R414H, that each

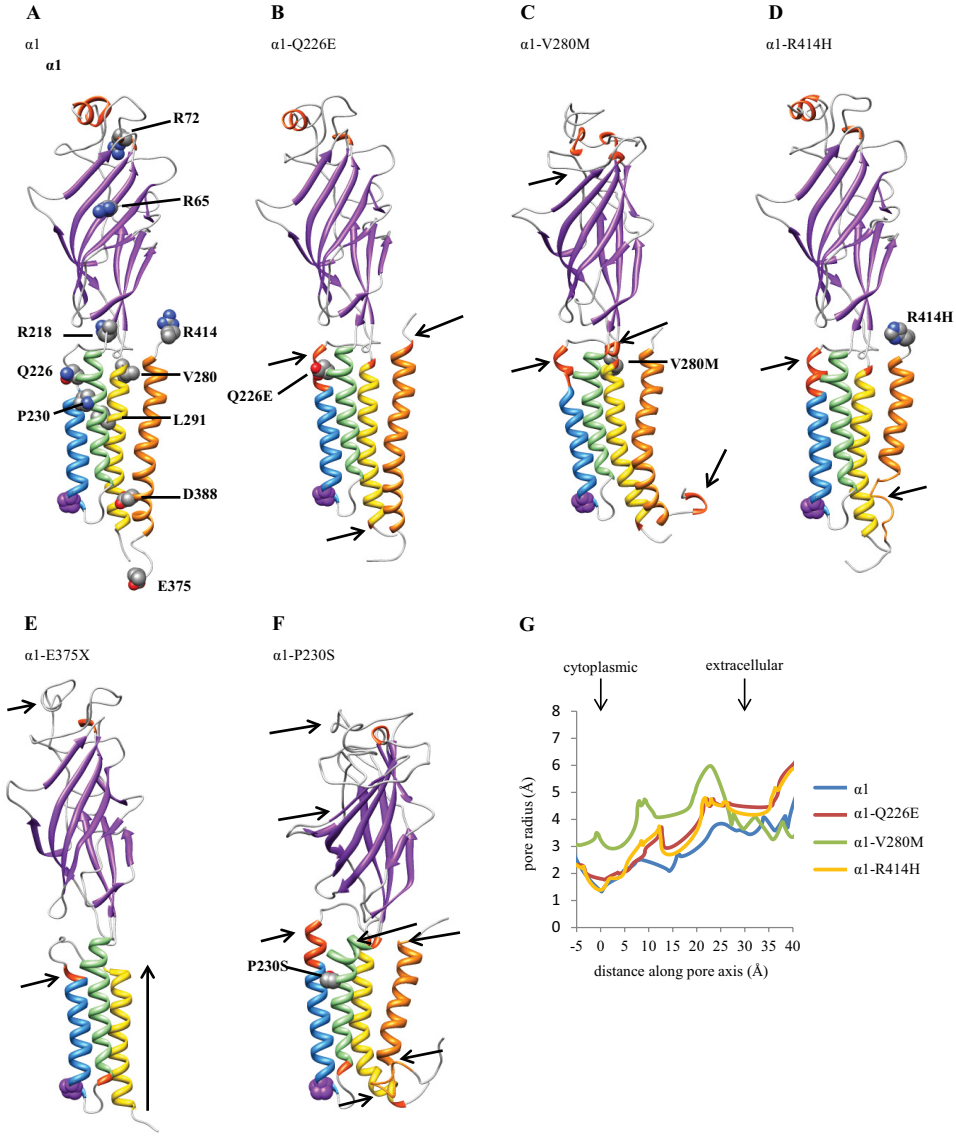

FIGURE 7. **Structural modeling of novel mutations.** *A–F*, major conformational changes compared with wild type receptors are indicated by *arrows*. TM1 is shown in *green*, TM2 is in *blue*, TM3 is in *yellow*, TM4 is in *orange*, 0′ (Arg-252) is in *purple*, and helical extensions are in *red*. *G*, pore radius for wild type and three novel autosomal dominant mutations. *Arrows* indicate the limits of the membrane.

produced spontaneously active channels. Prior to this study, only one hyperekplexia mutation (Y128C) was known to produce spontaneous activity (10). This mutation was also autosomal dominant. Spontaneous activity was evident not only in mutated homomeric channels, but also in channels formed by the co-expression of mutated subunits and α1 wild type subunits and/or β wild type subunits (Figs. 1 and 2). Structural modeling predicted that the mutations p.Q226E and p.V280M cause a widening of the outer channel pore, leading to spontaneous activity. The p.V280M mutation dramatically increased both the level of spontaneous activity and glycine sensitivity, suggesting a drastic destabilization of the closed channel state. The loss of the β sheet structure around the constraining loop C glycine-binding domain is likely to impact upon glycine binding and retention, rendering the glycine-binding site much more accessible. The kink introduced by p.V280M to the cytoplasmic end of the TM3 domain affects the close TM2-TM3 packing, reducing the stability of the closed channel, because of greater conformational freedom at the cytoplasmic end of the TM2 domain. Given that p.V280M-containing GlyRs expressed strongly at the cell surface (Fig. 6), the high level of spontaneous activity may partly explain the observed reduction in peak glycine-induced current magnitude. A reduction in the glycine-inducible current magnitude, coupled with a possible diminution of the chloride electrochemical gradient caused by the high level of spontaneous activity, may be among the mechanisms by which the p.V280M mutation disrupts glycinergic signaling.

In contrast, the glycine sensitivities of p.Q226E- and p.R414H-containing receptors were similar to that of wild type receptors, and both mutations caused spontaneous activity. However, modest reductions in the single-channel conductance and the cell surface expression efficiency would have reduced the chloride flux carrying capacity of p.Q226E-containing GlyRs and therefore may have contributed to the hyperekplexia phenotype (Figs. 2*D* and 6). Given that p.Q226E is closely apposed with p.R271 of the adjacent subunit, we

hypothesize that the enhanced electrostatic attraction between these oppositely charged residues may be responsible for the tonic receptor activity. In the p.R414H GlyR, the extremely low spontaneous open probability seems unlikely to have caused a hyperekplexia phenotype on its own, because the expression efficiency and glycine sensitivity were not diminished relative to that of wild type receptors. One possibility is that the mutation altered TM4 orientation and thus TM3-TM4 loop structure, leading to a change in propensity of this subunit to bind clustering proteins at synapses. No effect on the predicted structure of the extracellular domain fits with wild type comparable glycine sensitivity seen for this mutation. However, the main difference to the wild type monomer is the loss of α-helical structure at the cytoplasmic end of the TM4 domain. This region is at the outside of the pentamer and contains an unusually high proportion of charged residues for a transmembrane region, ^{382}QRAKKIDKISR^{392}, which is completely disrupted in p.R414H receptors.

The recessive p.R72C, p.R218W, and p.E375X mutations all precluded the surface expression of mutated homomeric GlyRs (Figs. 1 and 4). However, when each mutated subunit was co-expressed with α1 wild type or α1 and β wild type subunits, robust glycine-activated currents were observed. Because the glycine sensitivity of the resultant p.E375X receptor was significantly decreased relative to homomeric α1 GlyRs, we infer that the p.E375X subunit was incorporated into functional receptors together with either α1 subunits alone or with α1 plus β subunits. Because this result was unexpected, it was substantiated using voltage clamp fluorometry (Fig. 4*E*). We also attempted to confirm it using immunofluorescence, but the incorporation rate may have been too low to allow surface expression to be detected. As noted above, we were surprised that the p.E375X subunit was incorporated, given that previous studies have shown that TM4 deletion is incompatible with the surface expression of functional α1 GlyRs (32–35). Indeed, the deletion of only a few residues at the C-terminal end of the TM4 domain is sufficient to render some pLGIC receptors completely nonfunctional (12, 44, 45).

To our knowledge, this is the first suggestion that a pLGIC receptor subunit may be functionally expressed without a TM4 domain. The human GlyR α4 subunit (Uniprot accession number Q5JXX5) has long been regarded as a pseudo-gene because it incorporates a stop codon that truncates the receptor prior to the TM4 domain (3). The truncation occurs at residue Asp-383, which corresponds to Gln-382 in the α1 subunit. Because this is C-terminal of E375, it is possible that the α4 subunit may be incorporated into functional GlyRs, suggesting that it could exert a physiological role in modulating the functional properties of GlyRs. There may also be a case to reassess the pathophysiology of the other pLGIC late protein truncating events in epilepsy and related disorders, for example $GABA_A$ receptor mutations (46).

Genetic analysis suggested possible heterozygosity between p.R65W and p.P230S, although parental DNA was not available to confirm this. We previously described p.R65W as recessive on the basis of both the genetic analysis and a trafficking defect when expressed in the homozygous state (10). The present study shows that GlyRs comprised of p.R65W plus α1 and β wild type subunits exhibited a 20-fold increase in the glycine EC_{50} value (Figs. 1 and 5). Because this reduction in glycine sensitivity should be enough to cause hyperekplexia on its own (47, 48), it implies that the p.R65W mutation should be inherited in an autosomal dominant manner. It therefore remains a mystery why heterozygous parents remain asymptomatic, possibly implying the existence of compensating physiological mechanisms. The p.P230S mutation produced fast desensitizing receptors, reduced peak glycine-activated current magnitude, and modestly reduced glycine sensitivity (Figs. 1 and 5). All of these effects remained when the mutated subunit was co-expressed with α1 and/or β wild type subunits, implying that p.P230S should also exhibit an autosomal dominant inheritance mode. As expected, when p.R65W, p.P230S, and β wild type subunits were co-expressed to mimic compound heterozygosity, glycine sensitivity and peak current magnitudes were drastically reduced (Fig. 1, *A* and *C*), readily accounting for the hyperekplexia phenotype.

Because Arg-65 forms a crucial component of the glycine-binding site (5, 49), the nonconservative p.R65W mutation most likely disrupts glycine binding when functionally expressed with wild type subunits. Our finding that it is not trafficked to the surface when expressed as a homomer (Fig. 1) is most likely the result of a global structural disruption caused by this mutation (10). Because GlyR desensitization involves a specific conformational change at the extracellular domain-transmembrane domain interface (50), the effect of the p.P230S mutation on desensitization may be due to a conformational change at this interface.

Genetic analysis confirmed that the p.L291P and p.D388A mutations exhibited compound heterozygosity. Our functional analyses revealed that both mutated subunits did not express as homomers and exhibited reduced glycine sensitivity when individually co-expressed as heteromers with α1 and β wild type subunits (Figs. 1 and 5). We were unable to detect functional surface expression following co-expression of both p.L291P and p.D388A with β wild type subunits, which would account for the hyperekplexia phenotype.

In conclusion, this study illustrates the importance of hyperekplexia mutations in identifying new insights into the structure and function of GlyRs and other pLGIC family members. This in turn allows us to provide a more definitive explanation of the phenotype and clinical impact of the gene-positive patients through stratification of disease mechanisms.

Acknowledgment—We thank Dr. Han Lu for help with the voltage clamp fluorometry experiments.

REFERENCES

1. Lynch, J. W. (2004) Molecular structure and function of the glycine receptor chloride channel. *Physiol. Rev.* **84,** 1051–1095
2. Corringer, P. J., Baaden, M., Bocquet, N., Delarue, M., Dufresne, V., Nury, H., Prevost, M., and Van Renterghem, C. (2010) Atomic structure and dynamics of pentameric ligand-gated ion channels. New insight from bacterial homologues. *J. Physiol.* **588,** 565–572
3. Simon, J., Wakimoto, H., Fujita, N., Lalande, M., and Barnard, E. A. (2004) Analysis of the set of $GABA_A$ receptor genes in the human genome. *J. Biol. Chem.* **279,** 41422–41435
4. Yang, Z., Taran, E., Webb, T. I., and Lynch, J. W. (2012) Stoichiometry and

subunit arrangement of $\alpha 1\beta$ glycine receptors as determined by atomic force microscopy. *Biochemistry* **51,** 5229–5231
5. Grudzinska, J., Schemm, R., Haeger, S., Nicke, A., Schmalzing, G., Betz, H., and Laube, B. (2005) The β subunit determines the ligand binding properties of synaptic glycine receptors. *Neuron* **45,** 727–739
6. Lynch, J. W. (2009) Native glycine receptor subtypes and their physiological roles. *Neuropharmacology* **56,** 303–309
7. Bakker, M. J., van Dijk, J. G., van den Maagdenberg, A. M., and Tijssen, M. A. (2006) Startle syndromes. *Lancet Neurol.* **5,** 513–524
8. Davies, J. S., Chung, S. K., Thomas, R. H., Robinson, A., Hammond, C. L., Mullins, J. G., Carta, E., Pearce, B. R., Harvey, K., Harvey, R. J., and Rees, M. I. (2010) The glycinergic system in human startle disease. A genetic screening approach. *Front. Mol. Neurosci.* **3,** 8
9. Chung, S. K., Bode, A., Cushion, T. D., Thomas, R. H., Hunt, C., Wood, S. E., Pickrell, W. O., Drew, C. J., Yamashita, S., Shiang, R., Leiz, S., Longhardt, A. C., Raile, V., Weschke, B., Puri, R. D., Verma, I. C., Harvey, R. J., Ratnasinghe, D. D., Parker, M., Rittey, C., Masri, A., Lingappa, L., Howell, O. W., Vanbellinghen, J. F., Mullins, J. G., Lynch, J. W., and Rees, M. I. (2013) GLRB is the third major gene of effect in hyperekplexia. *Hum. Mol. Genet.* **22,** 927–940
10. Chung, S. K., Vanbellinghen, J. F., Mullins, J. G., Robinson, A., Hantke, J., Hammond, C. L., Gilbert, D. F., Freilinger, M., Ryan, M., Kruer, M. C., Masri, A., Gurses, C., Ferrie, C., Harvey, K., Shiang, R., Christodoulou, J., Andermann, F., Andermann, E., Thomas, R. H., Harvey, R. J., Lynch, J. W., and Rees, M. I. (2010) Pathophysiological mechanisms of dominant and recessive GLRA1 mutations in hyperekplexia. *J. Neurosci.* **30,** 9612–9620
11. James, V. M., Bode, A., Chung, S. K., Gill, J. L., Nielsen, M., Cowan, F. M., Vujic, M., Thomas, R. H., Rees, M. I., Harvey, K., Keramidas, A., Topf, M., Ginjaar, I., Lynch, J. W., and Harvey, R. J. (2013) Novel missense mutations in the glycine receptor β subunit gene (GLRB) in startle disease. *Neurobiol. Dis.* **52,** 137–149
12. Butler, A. S., Lindesay, S. A., Dover, T. J., Kennedy, M. D., Patchell, V. B., Levine, B. A., Hope, A. G., and Barnes, N. M. (2009) Importance of the C-terminus of the human 5-HT3A receptor subunit. *Neuropharmacology* **56,** 292–302
13. Chen, X., Webb, T. I., and Lynch, J. W. (2009) The M4 transmembrane segment contributes to agonist efficacy differences between $\alpha 1$ and $\alpha 3$ glycine receptors. *Mol. Membr. Biol.* **26,** 321–332
14. Harvey, K., Duguid, I. C., Alldred, M. J., Beatty, S. E., Ward, H., Keep, N. H., Lingenfelter, S. E., Pearce, B. R., Lundgren, J., Owen, M. J., Smart, T. G., Lüscher, B., Rees, M. I., and Harvey, R. J. (2004) The GDP-GTP exchange factor collybistin. An essential determinant of neuronal gephyrin clustering. *J. Neurosci.* **24,** 5816–5826
15. Rees, M. I., Harvey, K., Pearce, B. R., Chung, S. K., Duguid, I. C., Thomas, P., Beatty, S., Graham, G. E., Armstrong, L., Shiang, R., Abbott, K. J., Zuberi, S. M., Stephenson, J. B., Owen, M. J., Tijssen, M. A., van den Maagdenberg, A. M., Smart, T. G., Supplisson, S., and Harvey, R. J. (2006) Mutations in the gene encoding GlyT2 (SLC6A5) define a presynaptic component of human startle disease. *Nat. Genet.* **38,** 801–806
16. Rees, M. I., Harvey, K., Ward, H., White, J. H., Evans, L., Duguid, I. C., Hsu, C. C., Coleman, S. L., Miller, J., Baer, K., Waldvogel, H. J., Gibbon, F., Smart, T. G., Owen, M. J., Harvey, R. J., and Snell, R. G. (2003) Isoform heterogeneity of the human gephyrin gene (GPHN), binding domains to the glycine receptor, and mutation analysis in hyperekplexia. *J. Biol. Chem.* **278,** 24688–24696
17. Thomas, R. H., Chung, S. K., Wood, S. E., Cushion, T. D., Drew, C. J., Hammond, C. L., Vanbellinghen, J. F., Mullins, J. G., and Rees, M. I. (2013) Genotype-phenotype correlations in hyperekplexia. Apnoeas, learning difficulties and speech delay. *Brain* **136,** 3085–3095
18. Thomas, R. H., Harvey, R. J., and Rees, M. I. (2010) Hyperekplexia. Stiffness, startle and syncope. *J. Pediatr. Neurol.* **8,** 11–14
19. Engel, A. G., Ohno, K., Bouzat, C., Sine, S. M., and Griggs, R. C. (1996) End-plate acetylcholine receptor deficiency due to nonsense mutations in the epsilon subunit. *Ann. Neurol.* **40,** 810–817
20. Kruger, W., Gilbert, D., Hawthorne, R., Hryciw, D. H., Frings, S., Poronnik, P., and Lynch, J. W. (2005) A yellow fluorescent protein-based assay for high-throughput screening of glycine and GABAA receptor chloride channels. *Neurosci. Lett* **380,** 340–345
21. Pless, S. A., Dibas, M. I., Lester, H. A., and Lynch, J. W. (2007) Conformational variability of the glycine receptor M2 domain in response to activation by different agonists. *J. Biol. Chem.* **282,** 36057–36067
22. Hibbs, R. E., and Gouaux, E. (2011) Principles of activation and permeation in an anion-selective Cys-loop receptor. *Nature* **474,** 54–60
23. Grünberg, R., Nilges, M., and Leckner, J. (2007) Biskit. A software platform for structural bioinformatics. *Bioinformatics* **23,** 769–770
24. Wheeler, D. L., Barrett, T., Benson, D. A., Bryant, S. H., Canese, K., Chetvernin, V., Church, D. M., Dicuccio, M., Edgar, R., Federhen, S., Feolo, M., Geer, L. Y., Helmberg, W., Kapustin, Y., Khovayko, O., Landsman, D., Lipman, D. J., Madden, T. L., Maglott, D. R., Miller, V., Ostell, J., Pruitt, K. D., Schuler, G. D., Shumway, M., Sequeira, E., Sherry, S. T., Sirotkin, K., Souvorov, A., Starchenko, G., Tatusov, R. L., Tatusova, T. A., Wagner, L., and Yaschenko, E. (2008) Database resources of the National Center for Biotechnology Information. *Nucleic Acids Res.* **36,** D13–D21
25. Notredame, C., Higgins, D. G., and Heringa, J. (2000) T-Coffee. A novel method for fast and accurate multiple sequence alignment. *J. Mol. Biol.* **302,** 205–217
26. Eswar, N., John, B., Mirkovic, N., Fiser, A., Ilyin, V. A., Pieper, U., Stuart, A. C., Marti-Renom, M. A., Madhusudhan, M. S., Yerkovich, B., and Sali, A. (2003) Tools for comparative protein structure modeling and analysis. *Nucleic Acids Res.* **31,** 3375–3380
27. Pettersen, E. F., Goddard, T. D., Huang, C. C., Couch, G. S., Greenblatt, D. M., Meng, E. C., and Ferrin, T. E. (2004) UCSF Chimera. A visualization system for exploratory research and analysis. *J. Comput Chem* **25,** 1605–1612
28. Rees, M. I., Lewis, T. M., Vafa, B., Ferrie, C., Corry, P., Muntoni, F., Jungbluth, H., Stephenson, J. B., Kerr, M., Snell, R. G., Schofield, P. R., and Owen, M. J. (2001) Compound heterozygosity and nonsense mutations in the α_1-subunit of the inhibitory glycine receptor in hyperekplexia. *Hum. Genet.* **109,** 267–270
29. Brune, W., Weber, R. G., Saul, B., von Knebel Doeberitz, M., Grond-Ginsbach, C., Kellerman, K., Meinck, H. M., and Becker, C. M. (1996) A GLRA1 null mutation in recessive hyperekplexia challenges the functional role of glycine receptors. *Am. J. Hum. Genet.* **58,** 989–997
30. Beato, M., Groot-Kormelink, P. J., Colquhoun, D., and Sivilotti, L. G. (2002) Openings of the rat recombinant $\alpha 1$ homomeric glycine receptor as a function of the number of agonist molecules bound. *J. Gen. Physiol.* **119,** 443–466
31. Islam, R., and Lynch, J. W. (2012) Mechanism of action of the insecticides, lindane and fipronil, on glycine receptor chloride channels. *Br. J. Pharmacol.* **165,** 2707–2720
32. Haeger, S., Kuzmin, D., Detro-Dassen, S., Lang, N., Kilb, M., Tsetlin, V., Betz, H., Laube, B., and Schmalzing, G. (2010) An intramembrane aromatic network determines pentameric assembly of Cys-loop receptors. *Nat. Struct. Mol. Biol.* **17,** 90–98
33. Kling, C., Koch, M., Saul, B., and Becker, C. M. (1997) The frameshift mutation oscillator (Glra1(spd-ot)) produces a complete loss of glycine receptor $\alpha 1$-polypeptide in mouse central nervous system. *Neuroscience* **78,** 411–417
34. Unterer, B., Becker, C. M., and Villmann, C. (2012) The importance of TM3–4 loop subdomains for functional reconstitution of glycine receptors by independent domains. *J. Biol. Chem.* **287,** 39205–39215
35. Villmann, C., Oertel, J., Ma-Högemeier, Z. L., Hollmann, M., Sprengel, R., Becker, K., Breitinger, H. G., and Becker, C. M. (2009) Functional complementation of Glra1(spd-ot), a glycine receptor subunit mutant, by independently expressed C-terminal domains. *J. Neurosci.* **29,** 2440–2452
36. Pless, S. A., and Lynch, J. W. (2008) Illuminating the structure and function of Cys-loop receptors. *Clin. Exp. Pharmacol. Physiol.* **35,** 1137–1142
37. Langosch, D., Laube, B., Rundström, N., Schmieden, V., Bormann, J., and Betz, H. (1994) Decreased agonist affinity and chloride conductance of mutant glycine receptors associated with human hereditary hyperekplexia. *EMBO J.* **13,** 4223–4228
38. Lynch, J. W., Rajendra, S., Pierce, K. D., Handford, C. A., Barry, P. H., and Schofield, P. R. (1997) Identification of intracellular and extracellular domains mediating signal transduction in the inhibitory glycine receptor chloride channel. *EMBO J.* **16,** 110–120
39. Rajendra, S., Lynch, J. W., Pierce, K. D., French, C. R., Barry, P. H., and

Schofield, P. R. (1994) Startle disease mutations reduce the agonist sensitivity of the human inhibitory glycine receptor. *J. Biol. Chem.* **269,** 18739–18742
40. Saul, B., Kuner, T., Sobetzko, D., Brune, W., Hanefeld, F., Meinck, H. M., and Becker, C. M. (1999) Novel GLRA1 missense mutation (P250T) in dominant hyperekplexia defines an intracellular determinant of glycine receptor channel gating. *J. Neurosci.* **19,** 869–877
41. Humeny, A., Bonk, T., Becker, K., Jafari-Boroujerdi, M., Stephani, U., Reuter, K., and Becker, C. M. (2002) A novel recessive hyperekplexia allele GLRA1 (S231R). Genotyping by MALDI-TOF mass spectrometry and functional characterisation as a determinant of cellular glycine receptor trafficking. *Eur. J. Hum. Genet.* **10,** 188–196
42. Rea, R., Tijssen, M. A., Herd, C., Frants, R. R., and Kullmann, D. M. (2002) Functional characterization of compound heterozygosity for GlyRα1 mutations in the startle disease hyperekplexia. *Eur. J. Neurosci.* **16,** 186–196
43. Villmann, C., Oertel, J., Melzer, N., and Becker, C. M. (2009) Recessive hyperekplexia mutations of the glycine receptor α1 subunit affect cell surface integration and stability. *J. Neurochem.* **111,** 837–847
44. Estrada-Mondragón, A., Reyes-Ruiz, J. M., Martínez-Torres, A., and Miledi, R. (2010) Structure-function study of the fourth transmembrane segment of the GABArho1 receptor. *Proc. Natl. Acad. Sci. U.S.A.* **107,** 17780–17784
45. Pons, S., Sallette, J., Bourgeois, J. P., Taly, A., Changeux, J. P., and Devillers-Thiéry, A. (2004) Critical role of the C-terminal segment in the maturation and export to the cell surface of the homopentameric α7–5HT3A receptor. *Eur. J. Neurosci.* **20,** 2022–2030
46. Kang, J. Q., Shen, W., Lee, M., Gallagher, M. J., and Macdonald, R. L. (2010) Slow degradation and aggregation in vitro of mutant GABAA receptor γ2(Q351X) subunits associated with epilepsy. *J. Neurosci.* **30,** 13895–13905
47. Graham, B. A., Schofield, P. R., Sah, P., Margrie, T. W., and Callister, R. J. (2006) Distinct physiological mechanisms underlie altered glycinergic synaptic transmission in the murine mutants spastic, spasmodic, and oscillator. *J. Neurosci.* **26,** 4880–4890
48. Ryan, S. G., Buckwalter, M. S., Lynch, J. W., Handford, C. A., Segura, L., Shiang, R., Wasmuth, J. J., Camper, S. A., Schofield, P., and O'Connell, P. (1994) A missense mutation in the gene encoding the α1 subunit of the inhibitory glycine receptor in the spasmodic mouse. *Nat. Genet.* **7,** 131–135
49. Pless, S. A., Millen, K. S., Hanek, A. P., Lynch, J. W., Lester, H. A., Lummis, S. C., and Dougherty, D. A. (2008) A cation-pi interaction in the binding site of the glycine receptor is mediated by a phenylalanine residue. *J. Neurosci.* **28,** 10937–10942
50. Wang, Q., and Lynch, J. W. (2011) Activation and desensitization induce distinct conformational changes at the extracellular-transmembrane domain interface of the glycine receptor. *J. Biol. Chem.* **286,** 38814–38824
51. Miraglia Del Giudice, E., Coppola, G., Bellini, G., Ledaal, P., Hertz, J. M., and Pascotto, A. (2003) A novel mutation (R218Q) at the boundary between the N-terminal and the first transmembrane domain of the glycine receptor in a case of sporadic hyperekplexia. *J. Med. Genet.* **40,** e71
52. Bellini, G., Miceli, F., Mangano, S., Miraglia del Giudice, E., Coppola, G., Barbagallo, A., Taglialatela, M., and Pascotto, A. (2007) Hyperekplexia caused by dominant-negative suppression of glyra1 function. *Neurology* **68,** 1947–1949
53. Vergouwe, M. N., Tijssen, M. A., Peters, A. C., Wielaard, R., and Frants, R. R. (1999) Hyperekplexia phenotype due to compound heterozygosity for GLRA1 gene mutations. *Ann. Neurol.* **46,** 634–638
54. Shiang, R., Ryan, S. G., Zhu, Y. Z., Hahn, A. F., O'Connell, P., and Wasmuth, J. J. (1993) Mutations in the α1 subunit of the inhibitory glycine receptor cause the dominant neurologic disorder, hyperekplexia. *Nat. Genet.* **5,** 351–358
55. Shiang, R., Ryan, S. G., Zhu, Y. Z., Fielder, T. J., Allen, R. J., Fryer, A., Yamashita, S., O'Connell, P., and Wasmuth, J. J. (1995) Mutational analysis of familial and sporadic hyperekplexia. *Ann. Neurol.* **38,** 85–91